Hindawi Publishing Corporation
Mathematical Problems in Engineering
Volume 2013, Article ID 980161, 10 pages
http://dx.doi.org/10.1155/2013/980161

Research Article

Development and Validation of an Enhanced Coupled-Field Model for PZT Cantilever Bimorph Energy Harvester

Long Zhang,[1] Keith A. Williams,[1] and Zhengchao Xie[2]

[1] *Department of Mechanical Engineering, The University of Alabama, Tuscaloosa, AL, USA*
[2] *Department of Electromechanical Engineering, Faculty of Science and Technology, University of Macau, Macau, China*

Correspondence should be addressed to Zhengchao Xie; zxie@umac.mo

Received 19 August 2012; Revised 2 January 2013; Accepted 16 January 2013

Academic Editor: Yuji Liu

The power source with the limited life span has motivated the development of the energy harvesters that can scavenge the ambient environment energy and convert it into the electrical energy. With the coupled field characteristics of structure to electricity, piezoelectric energy harvesters are under consideration as a means of converting the mechanical energy to the electrical energy, with the goal of realizing completely self-powered sensor systems. In this paper, two previous models in the literatures for predicting the open-circuit and close-circuit voltages of a piezoelectric cantilever bimorph (PCB) energy harvester are first described, that is, the mechanical equivalent spring mass-damper model and the electrical equivalent circuit model. Then, the development of an enhanced coupled field model for the PCB energy harvester based on another previous model in the literature using a conservation of energy method is presented. Further, the laboratory experiments are carried out to evaluate the enhanced coupled field model and the other two previous models in the literatures. The comparison results show that the enhanced coupled field model can better predict the open-circuit and close-circuit voltages of the PCB energy harvester with a proof mass bonded at the free end of the structure in order to increase the energy-harvesting level of the system.

1. Introduction

The past few years have seen the rapid development of small wireless sensor networks, which have considerable potential in areas ranging from building monitoring and environmental control to military applications. The associate electronics have traditionally relied on the use of electrochemical batteries for electrical energy [1]. The associated battery replacement requirements can be problematic: the economic cost may include not only the capital cost of the batteries themselves, but also the cost of the labor for performing replacement in remote or otherwise limited-access locations. In addition, in some applications, safety monitoring and fire protection, for example, serious problems may occur if batteries fail without warning. In an effort to address these problems, researchers [1–3] have explored technologies for obtaining electrical energy by converting ambient energy that is already available around the device, such as solar energy and temperature differentials. Solar energy, in particular, is a very attractive source for powering sensor networks and has become more mature over the years. However, certain limitations remain: the variation in light intensity can drop its efficiency significantly and the requisite surface area may limit its application to microsensor networks. Another approach is to harvest mechanical vibration energy present in an environment. Many environments are subjected to ambient vibration energy that is commonly unused. Methods for obtaining electrical energy from vibrations include the use of piezoelectric materials, electromagnetic induction, and electrostatic generation [4]. Piezoelectric transducers are suitable as kinetic energy to electrical energy converters due to their typically light-weight, high-adaptability, and high-energy densities [5–8]. As such, piezoelectric energy harvesters have received a great deal of attention from researchers in recent years.

Piezoelectric materials can be configured in many different ways that may prove useful in energy-harvesting applications. Perhaps the simplest and most widely used configuration is the piezoelectric cantilever bimorph (PCB). A PCB is typically a cantilevered metal beam with piezoelectric

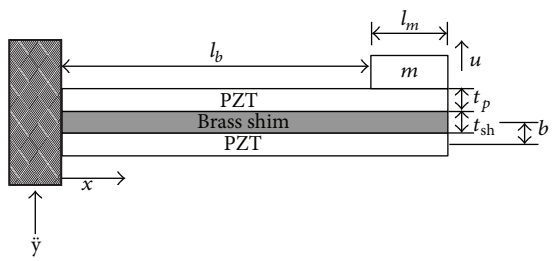

Figure 1: A schematic diagram of the PCB.

layers laminated on its top and bottom surfaces. Important potentials for the PCB structure include bonding the proof mass on the free end of the structure to increase the strain level of the piezoelectric layers and tuning the resonant frequency of the structure to that of ambient vibration to maximize the vibration level of the structure.

In this paper, two previous models, that is, a mechanical equivalent model and an electrical equivalent model, for predicting the open-circuit voltage and the close-circuit voltage of the PCB energy harvester are first described. Then an enhanced coupled field model of the PCB energy harvester is presented based on previous model in the literature using a conservation of energy method. Further, a prototype of the PCB energy harvester is then constructed for laboratory testing using a commercially available piezoelectric bimorph. The theoretical results of the above models are finally compared with the experimental results, in terms of the open-circuit voltage and close-circuit voltage of the PCB energy harvester.

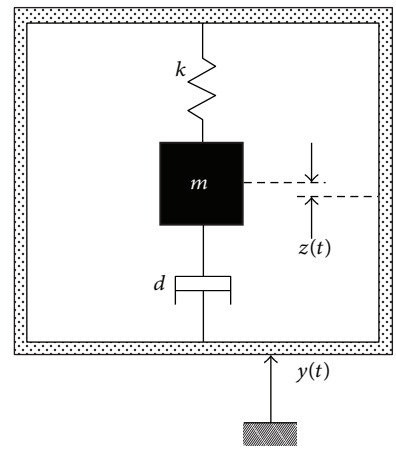

Figure 2: Schematic of general vibration converter model [8].

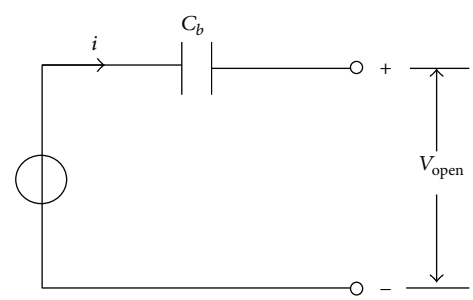

Figure 3: Open-circuit model of PZT energy harvester.

2. General Configuration of Piezoelectric Cantilever Bimorph

A typical PCB with the proof mass on the free end is shown in Figure 1. It consists of a central brass layer sandwiched by two PZT layers and the structure is clamped to the left end. Among the published works with the modeling of the PCB energy harvester, many have applied either a mechanical equivalent mass-spring-damper model or an electrical equivalent circuit model to represent the coupled field characteristics of the PCB energy harvester. The two previous models developed, respectively, by Williams and Yates [9] and Roundy and Wright [11] will be described concisely in the following section.

2.1. A Mechanical Equivalent Model Developed by Williams and Yates. Williams and Yates (1996) proposed a general model for the conversion of mechanical energy into the electrical energy, which can be used for modeling of piezoelectric, electromagnetic and electrostatic, generators. A schematic diagram of the generator is shown in Figure 2 [9].

According to Williams and Yates, the equation of motion of the model is described as follows:

$$m\ddot{z} + d\dot{z} + kz = -m\ddot{y}, \tag{1}$$

where z is tip displacement of PCB structure show in Figure 1, $\ddot{y}$ is input vibration acceleration, m is proof mass, d is damping constant, and k is spring constant respectively. The generated instantaneous power in the PZT bimorph is the product of the force on the beam and its velocity, as is given by

$$p(t) = F * [\dot{y}(t) + \dot{z}(t)] = -m\ddot{y} * [\dot{y}(t) + \dot{z}(t)]. \tag{2}$$

For sinusoidal vibration excitation, assume $y(t) = Y_0 * \cos(\omega t)$, and the generated electrical power can be found as follows:

$$|P(j\omega)| = \frac{m\zeta {Y_0}^2 \omega^3 (\omega/\omega_n)}{(1 - (\omega^2/{\omega_n}^2))^2 + (2\zeta(\omega/\omega_n))^2}, \tag{3}$$

where ζ is the damping ratio and ω_n is the fundamental resonant frequency of PCB structure. If PCB energy harvester works at its resonant frequency, the generated power can be simplified as

$$|P(j\omega)| = \frac{m{Y_0}^2\omega^3}{4\zeta}. \tag{4}$$

The open-circuit voltage, close-circuit load voltage, and power can then be derived from (4). According to Park [10], the best-fit circuit model of PZT sensor is a voltage generator connected in series with a capacitor, as is shown in Figure 3, where C_b is the inner capacitance of PCB.

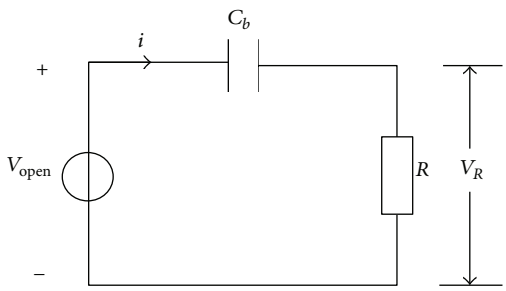

Figure 4: Close-circuit model of PZT energy harvester.

The open-circuit voltage is assumed as $u(t) = \sqrt{2} * U * \sin(\omega_n t)$, where U is the RMS value of alternating voltage. The alternating current can then be obtained as follows:

$$i(t) = \frac{dQ(t)}{dt} = C_b * \frac{du(t)}{dt} = \sqrt{2} C_b \omega_n U * \cos(\omega_n t). \quad (5)$$

The reactive instantaneous power consumed by capacitor is given by

$$P = -U_{\text{eff}} * I_{\text{eff}} = -U * C_b \omega_n U = -C_b \omega_n U^2, \quad (6)$$

where U_{eff} and I_{eff} represent the RMS values of alternating voltage and current. Substitute (5) into (4), and then the RMS value of open-circuit voltage can be obtained as follows:

$$U = \sqrt{\frac{m Y_0{}^2 \omega_n{}^2}{4\zeta C_b}} = \frac{Y_0 \omega_n}{2} \sqrt{\frac{m}{\zeta C_b}}. \quad (7)$$

Hence, the open-circuit voltage is given by

$$u(t) = \sqrt{2} U \sin(\omega_n t) = Y_0 \omega_n \sqrt{\frac{m}{2\zeta C_b}} \sin(\omega_n t). \quad (8)$$

For the close circuit, piezoelectric generator is connected with resistive load in series, as is shown in Figure 4.

The open-circuit voltage of piezoelectric generator can be expressed in the form of complex number by $u(t) = U\angle 0^\circ$. The total impedance in the close circuit is given by

$$Z = R + \frac{1}{j\omega_n c} = \sqrt{R^2 + \frac{1}{\omega_n{}^2 C_b{}^2}} \angle -\varphi, \quad (9)$$

where $\varphi = \tan^{-1}(1/\omega_n C_b R)$. By the use of the voltage divider principle, the voltage of resistive load can then be found as follows:

$$u_R = \frac{R}{Z} u(t) = \frac{\omega_n C_b R}{\sqrt{1 + \omega_n{}^2 C_b{}^2 R^2}} U\angle\varphi. \quad (10)$$

Hence, the close-circuit voltage on the resistive load is given by

$$u_R(t) = \sqrt{2} * \frac{\omega_n C_b R}{\sqrt{1 + \omega_n{}^2 C_b{}^2 R^2}} U \sin(\omega_n t + \varphi). \quad (11)$$

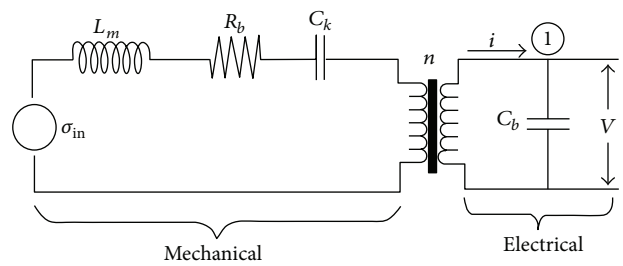

Figure 5: Circuit representation of the piezoelectric generator [10].

The power consumed by the resistive load can then be obtained as follows:

$$P_R = \frac{U_{R_{\text{eff}}}{}^2}{R} = \frac{\left(U\omega_n C_b R / \sqrt{1 + \omega_n{}^2 C_b{}^2 R^2}\right)^2}{R} = \frac{\omega_n{}^2 C_b{}^2 R}{1 + \omega_n{}^2 C_b{}^2 R^2} U^2, \quad (12)$$

where $U_{R_{\text{eff}}}$ represents the RMS value of the alternating voltage of resistive load. From (12), the optimal value of R for the maximum power output of PCB power generator can then found to be

$$R_{\text{opt}} = \frac{1}{\omega_n C_b}. \quad (13)$$

2.2. An Electrical Equivalent Circuit Model Developed by Roundy (2003). An electrical equivalent circuit model that models both mechanical and electrical portions of the piezoelectric system as circuit elements is a convenient method to study the characteristics of piezoelectric energy harvester. An equivalent circuit representation of PCB energy harvester developed by Roundy is shown in Figure 5 [11], where σ_{in} represents stress generator excited by input vibration, inductor L_m represents the mass of the generator, resistor R_b represents the mechanical damping, capacitor C_k represents the mechanical stiffness, n represents the turns of transformer, which represents the electromechanical coupling of PCB, C_b represents the inner capacitance of PCB, and V represents the open-circuit voltage.

The generated voltage with resistive load was derived by Roundy [10], as is shown in the following equation:

$$V = \frac{j2\omega c_p d_{31} t_p}{(a\varepsilon k_2)} \times \left(\frac{\omega_n{}^2}{RC_b} - \left(\frac{1}{RC_b} + 2\zeta\omega_n \right) \omega^2 + j\omega \left[\omega_n{}^2 \left(1 + k_{31}{}^2\right) + \frac{2\zeta\omega_n}{RC_b} - \omega^2 \right] \right)^{-1}, \quad (14)$$

where $k_2 = L_b{}^2(3L_m + 4L_b)/[3(L_b + L_m)(t_{\text{sh}} + t_p)]$, $k_{31} = d_{31}{}^2 c_p/\varepsilon$ is the coupling coefficient of PCB, ω and ω_n are the driving frequency and resonant frequency of PCB, c_p, L_b, t_p, ε, and d_{31} are Young's modules, effective length, thickness, dielectric constant, and strain coefficient of the

single piezoelectric layer, $a = 1$ if the two piezo layers are wired in series and $a = 2$ if they are wired in parallel, c_{sh} and t_{sh} are Young's modules and thickness of central brass shim, L_m is the length of the proof mass, A_{in} is the ambient vibration amplitude, R is the resistive load, ζ is the damping ratio, is the coupling coefficient. The open-circuit voltage can be obtained by making the resistive load value infinitely large.

If the driving frequency ω of the input vibration matches the resonant frequency ω_n of PCB generator and the load is resistive, the RMS power transferred to the load and the optimal load resistance can be found as follows [10]:

$$P = \frac{1}{2\omega_n^2} \frac{RC_b^2\left(2c_p d_{31} t_p\right)^2 / \left(k_2 a\varepsilon\right)^2 A_{in}^2}{\left(4\zeta^2 + k_{31}^4\right)\left(RC_b\omega_n\right)^2 + 4\zeta k_{31}^2\left(RC_b\omega_n\right) + 4\zeta^2},$$
$$R_{opt} = \frac{1}{\omega_n C_b} \frac{2\zeta}{\sqrt{4\zeta^2 + k_{31}^4}}. \tag{15}$$

2.3. An Enhanced Coupled Field Model by a Conservation of Energy Method. Roundy and Wright [11] and Wang et al. [12] derived an analytical expression for the generated voltage of piezoelectric triple layer bender to the applied mechanical input excitations, including moment M, tip force F, and body force p. The method is based on the internal energy for the thermodynamic equilibrium. Kim [13] used the same principle to study the voltage generation of unimorph, interdigitated unimorph, bimorph and interdigitated bimorph cantilever bender, and diaphragm. Ng [14] and Ajitsaria [15] studied voltage generation of cantilever bimorph with a proof mass at the free end based on Wang and Kim's derivation. Among these studies, however, the effect of the proof mass on the piezoelectric effect of the bimorph was not fully taken into consideration.

According to the finite element analysis (FEA) of the PCB structure with proof mass on the free end, the equivalent strain distribution under the proof mass is shown in Figure 6. Due to the high rigidity of the proof mass, which is bonded onto the free end of the PZT bimorph, the equivalent strain under the proof mass is minimal and negligible, as compared with other PZT parts. As a result, minimal and negligible piezoelectric effect will be expected to occur at the PZT parts under the proof mass. In addition, under the extreme condition that the proof mass is long enough to cover the most areas of the PZT bimorph, the PCB energy harvester will certainly not produce much electrical energy, as is not taken into considerations among the previous models in the literature. Therefore, in the following enhanced coupled field modeling of the PCB energy harvest, it is assumed that the PZT parts under the proof mass do not contribute to the voltage generation of the PCB generator subjected to ambient vibration. In other words, the PZT material under the proof mass will be only treated as a rigid body and will not result in any piezoelectric effect. Further, a second assumption in the enhanced coupled field model is that the proof mass will be treated as a point mass when calculating its acting force on the bimorph.

The detailed derivation of the enhanced coupled field model based on Kim [13] for the voltage and power output of the PCB generator is presented next. The constitutive equations for the top and bottom PZT layer are expressed by the following equations:

The constitutive equations for upper and lower layers are can be expressed by the following equation.

$$S_1 = s_{11}\sigma_1 \mp d_{31}E_3,$$
$$D_3 = \mp d_{31}\sigma_1 + \varepsilon_{33}E_3, \tag{16}$$

where the two piezoelectric layers in the bimorph are poled in opposite directions. S_1 is the mechanical strain in the longitudinal direction, s_{11} is the compliance or the reciprocal of Young's modulus, σ_1 is the mechanical stress in the longitudinal direction, d_{31} is the piezoelectric strain coefficient, D_3 is electrical displacement in the transverse direction, and E_3 is the electrical field intensity.

The stress inside PZT material and central brass shim can then be obtained as

$$\sigma_1 = c_p\left(S_1 \pm d_{31}E_3\right),$$
$$\sigma_{sh} = c_{sh}S_1. \tag{17}$$

Because the bimorph is symmetric, the neutral surface is the middle surface of the brass shim. The relationship between strain and bimorph curvature ρ would be $S_1 = -\rho z$, where z represents the distance from the neutral surface. The moment in the bimorph can be calculated by the following expression [13]:

$$M = \int_{A_{upper}} \sigma_{1_{upper}} z\,dz + \int_{A_{sh}} \sigma_{sh} z\,dz + \int_{A_{lower}} \sigma_{1_{lower}} z\,dz. \tag{18}$$

Substituting (17) into (18),

$$M = \int_{t_{sh}/2}^{(t_{sh}/2)+t_p} c_p\left(-\rho z + d_{31}E_3\right) wz\,dz + \int_{-t_{sh}/2}^{t_{sh}/2} -c_{sh}\rho z\,wz\,dz$$
$$+ \int_{-((t_{sh}/2)+t_p)}^{-t_{sh}/2} c_p\left(-\rho z - d_{31}E_3\right) wz\,dz. \tag{19}$$

The equivalent excitation force induced by vibration acceleration is given by [14]:

$$F = -m\omega^2 Y * \sin(\omega t), \tag{20}$$

where m is the proof mass at the free end of bimorph, Y is the displacement amplitude of the center of proof mass, and ω is the driving frequency. The moment induced by excitation force is given by

$$M = F * \left(L_b + \frac{1}{2}L_m - x\right). \tag{21}$$

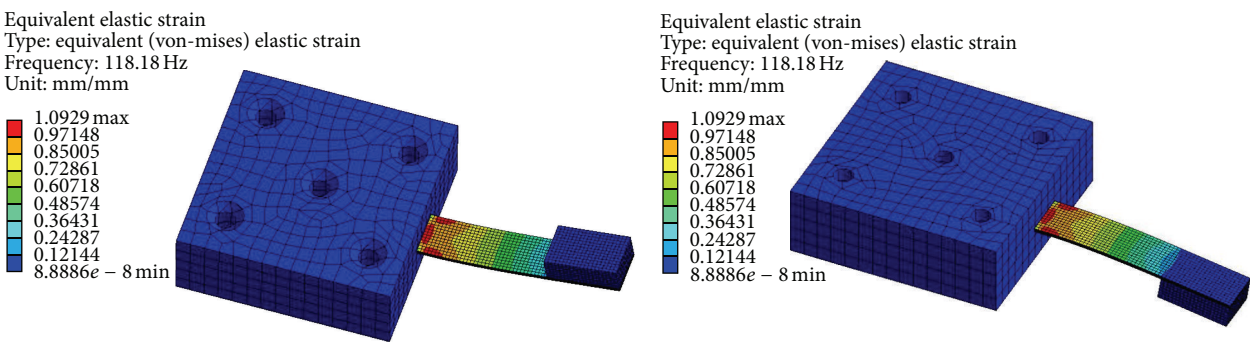

(a) (b)

Figure 6: Top and bottom surface equivalent strain of PCB generator.

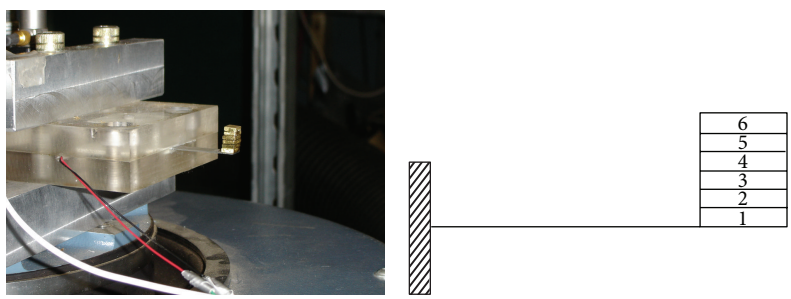

(a) (b)

Figure 7: PCB generator prototype and schematic test setup.

Combining (19) and (21), the curvature of the cantilever bimorph can be obtained as follows:

$$\rho = \frac{F}{g_1}\left(L_b + \frac{1}{2}L_m - x\right) - \frac{g_2}{g_1}E_3, \tag{22}$$

where $g_1 = -(2/3)c_p w(t_p{}^3 + (3/2)t_p{}^2 t_{\text{sh}} + (3/4)t_p t_{\text{sh}}{}^2) - (1/12)c_{\text{sh}} w * t_{\text{sh}}{}^3$, $g_2 = c_p w d_{31}(t_p{}^2 + t_p t_{\text{sh}})$.

According to thermodynamic equilibrium, the energy densities of the piezoelectric layer and the central brass shim are given by

$$\begin{aligned} dU_p &= \frac{1}{2}S_1\sigma_1 + \frac{1}{2}D_3E_3, \\ dU_{\text{sh}} &= \frac{1}{2}S_1\sigma_{\text{sh}}. \end{aligned} \tag{23}$$

Substitute (17) and (22) into (23), the energy densities of the bimorph cantilever are

$$\begin{aligned} dU_{p\text{-upper}} &= \frac{1}{2}c_p\rho^2z^2 + \left(-\frac{1}{2}c_p d_{31}{}^2 + \frac{1}{2}\varepsilon_{33}\right)E_3{}^2, \\ dU_{p\text{-lower}} &= \frac{1}{2}c_p\rho^2z^2 + \left(-\frac{1}{2}c_p d_{31}{}^2 + \frac{1}{2}\varepsilon_{33}\right)E_3{}^2, \\ dU_{\text{sh}} &= \frac{1}{2}c_{\text{sh}}\rho^2z^2. \end{aligned} \tag{24}$$

From (24), it can be seen that the energy density in the upper piezoelectric layer and that in the lower piezoelectric layer of the bimorph are identical to each other although they always operate in the different bending modes, that is, extending mode the compression mode. Thus, the total internal energy in the bimorph can be calculated by integrating the energy density over the system:

$$\begin{aligned} U = {} & \int_0^L \int_0^w \int_{t_{\text{sh}}/2}^{(t_{\text{sh}}/2)+t_p} dU_{\text{upper}}\,dz\,dy\,dx \\ & - \int_{L-L_m}^L \int_0^w \int_{t_{\text{sh}}/2}^{(t_{\text{sh}}/2)+t_p} \frac{1}{2}\left(\varepsilon_{33} - c_p d_{31}{}^2\right)E_3{}^2\,dz\,dy\,dx \\ & + \int_0^L \int_0^w \int_{-t_{\text{sh}}/2}^{t_{\text{sh}}/2} dU_{\text{sh}}\,dz\,dy\,dx \\ & + \int_0^L \int_0^w \int_{-((t_{\text{sh}}/2)+t_p)}^{-t_{\text{sh}}/2} dU_{\text{lower}}\,dz\,dy\,dx, \end{aligned} \tag{25}$$

where the second term of the right hand side of the equation indicates the energy of upper piezoelectric layer under the proof mass that is only composed of elastic energy, because the electrode of upper piezoelectric layer does not extend under the proof mass.

Table 1: Characteristics of Q220-A4-203Y [17].

Property	Units	Value
Length L	mm	28.43
Width w	mm	6.35
Piezo thickness t_p	mm	0.19
Central brass thickness t_{sh}	mm	0.13
Strain coefficient d_{31}	$\times 10^{-12}$ m/V	–190
Coupling coefficient k_{31}	CV/Nm	0.35
Young's modulus c_p	GPa	66

Table 2: Resonant frequency of PCB generators and proof mass displacements.

	1P	2P	3P	4P	5P	6P
Resonant frequency (Hz)	166.0	129.4	105.0	92.8	83.0	75.7
Center displacement of proof mass (μm)	291	403	463	496	633	688

Substituting (24) into (25), the energy of bimorph system can be obtained as follows:

$$U = \frac{F^2 w g_3}{24 g_1^2}\left(24 c_p g_5 + c_{sh} t_{sh}^3\right) - \frac{w g_2 g_4}{24 g_1^2}\left(24 c_p g_5 + c_{sh} t_{sh}^3\right) F * E_3 + \left[\frac{w g_2^2 L}{24 g_1^2}\left(24 c_p g_5 + c_{sh} t_{sh}^3\right) + \frac{1}{2}\left(\varepsilon_{33} - c_p d_{31}^2\right)(2L - L_m) t_p w\right] * E_3^2, \tag{26}$$

where $g_3 = (L_b + (1/2)L_m)^2 L - (L_b + (1/2)L_m)L^2 + (1/3)L^3$, $g_4 = 2(L_b + (1/2)L_m)L - L^2$ and $g_5 = (1/3)(t_p^3 + (3/2)t_p^2 t_{sh} + (3/4)t_p t_{sh}^2)$.

The two piezoelectric layers are wired for parallel operation; thus, $E_3 = V/t_p$, where V is the generated voltage between the top surface and the bottom surface of one piezoelectric layer. Substituting it into (26) and differentiating (26) with V gives the generated electrical charge:

$$Q = -\frac{w g_2 g_4}{48 g_1^2 t_p}\left(24 c_p g_5 + c_{sh} t_{sh}^3\right) * F + \left[\frac{w g_2^2 L}{48 g_1^2 t_p^2}\left(24 c_p g_5 + c_{sh} t_{sh}^3\right) + \frac{1}{4 t_p}\left(\varepsilon_{33} - c_p d_{31}^2\right)(2L - L_m) w\right] * V. \tag{27}$$

There are two terms in the right hand side of (27). The first term is the electrical charge induced by mechanical vibration, which can be represented by Q_m, and the second term is the static electrical charge stored in the bimorph, which cannot be output for energy harvesting.

The capacitance of the bimorph can be found by differentiating the generated electrical charge Q with V as follows:

$$C_b = \frac{\partial Q}{\partial V} = \frac{w g_2^2 L}{48 g_1^2 t_p^2}\left(24 c_p g_5 + c_{sh} t_{sh}^3\right) + \frac{1}{4 t_p}\left(\varepsilon_{33} - c_p d_{31}^2\right)(2L - L_m) w. \tag{28}$$

According to the relation $Q = CV$, the open-circuit voltage of PCB energy harvester can then be obtained as follows:

$$V_{open} = \frac{Q_m}{C_b} = \frac{-g_2 g_4 t_p\left(24 c_p g_5 + c_{sh} t_{sh}^3\right) m \omega_n^2 Y}{\left[g_2^2 L\left(24 c_p g_5 + c_{sh} t_{sh}^3\right) + 12 g_1^2 t_p\left(\varepsilon_{33} - c_p d_{31}^2\right)(2L - L_m)\right]} * \sin(\omega_n t). \tag{29}$$

The close-circuit voltage and resistive load power can be calculated by (11) and (12).

3. Experimental Procedure

A prototype of PCB generator shown in Figure 7(a) was built with a PZT bimorph Q220-A4-203Y from Piezo Systems. The characteristics of the bimorph are summarized in Table 1 [16]. The proof mass was made of brass with the dimension of 5.3 mm × 6.35 mm × 1.6 mm. At each test step, one piece of proof mass was added onto the free end of PCB, as is shown in Figure 7(b).

The prototype was excited by input vibration of 11.2 m/s^2 at the resonant frequency of the structure at each test setup. The center displacement of proof mass on the free end was measured by PSV-300 vibrometer, and the resonant frequency of the structure was obtained by fast fourier transform (FFT) of the sinusoidal sweep test data of open-circuit voltage, since the maximum voltage occurs at the resonant frequency of the generator, according to Roundy [4]. The damping ratio was determined by calculating the damped harmonic oscillation of open-circuit voltage caused by applying a vibration impulse to the PCB generator.

4. Results and Discussion

The enhanced coupled field model was first compared with the base model of Kim's derivation in the previous literature and the experimental results, and then it was also compared with the other two prior analytical models, that is, mechanical equivalent model and electrical equivalent model, in terms of both open-circuit voltage and close-circuit voltage. The resonant frequencies of the PCB generator with different number of proof mass, and the vertical displacements of the proof mass center are shown in Table 2, where "2P" means

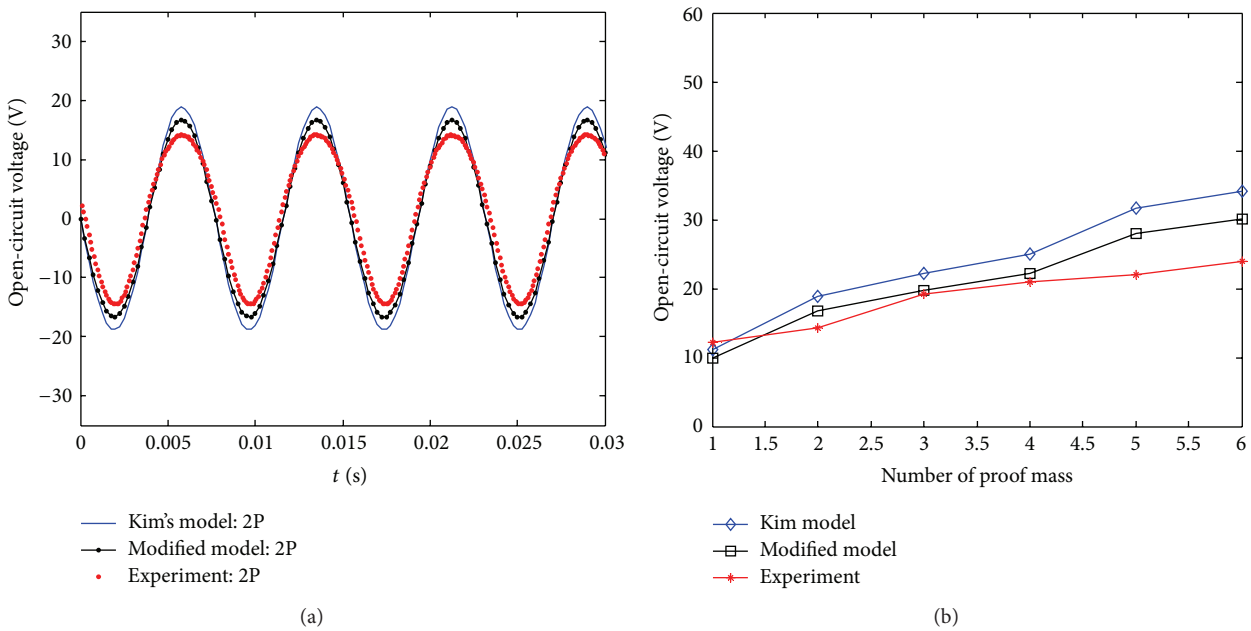

Figure 8: Open-circuit voltage of Kim's model and the enhanced model.

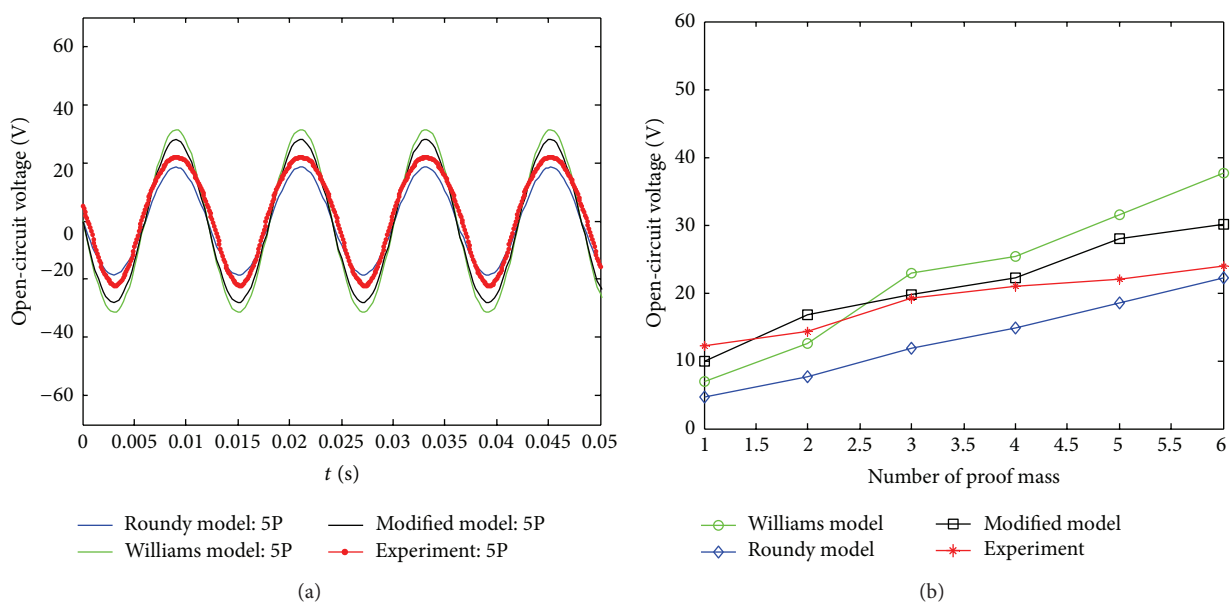

Figure 9: Open-circuit voltage of Williams's model, Roundy's model, and the enhanced coupled field model.

the PCB structure with "2" stacked proof mass bonded onto its free end. The average of the measured damping ratio of the PCB structure was 0.21. The resistive loads used for the experiment were 25, ranging from 1 KΩ to 1 MΩ.

4.1. Open-Circuit Voltage. The open-circuit voltage amplitude of the PCB generator with different proof mass is plotted in Figure 8, comparing the theoretical result of Kim's model, the enhanced coupled field model against the experimental results. It is clear that in Figure 8(b) the open-circuit voltage amplitude of the PCB generator increases with the number increase of the proof mass. In addition, the enhanced coupled field model is closer to the experimental result than Kim's model, since it treats the PZT parts under the proof mass as only the rigid body without piezoelectric effect, and it can better reflect the practical working mechanism of PCB generator with proof mass on the free end.

The open-circuit voltage of the enhanced coupled field model was also compared with that of Williams' model and Roundy's model, as shown in Figure 9. It is also clear that

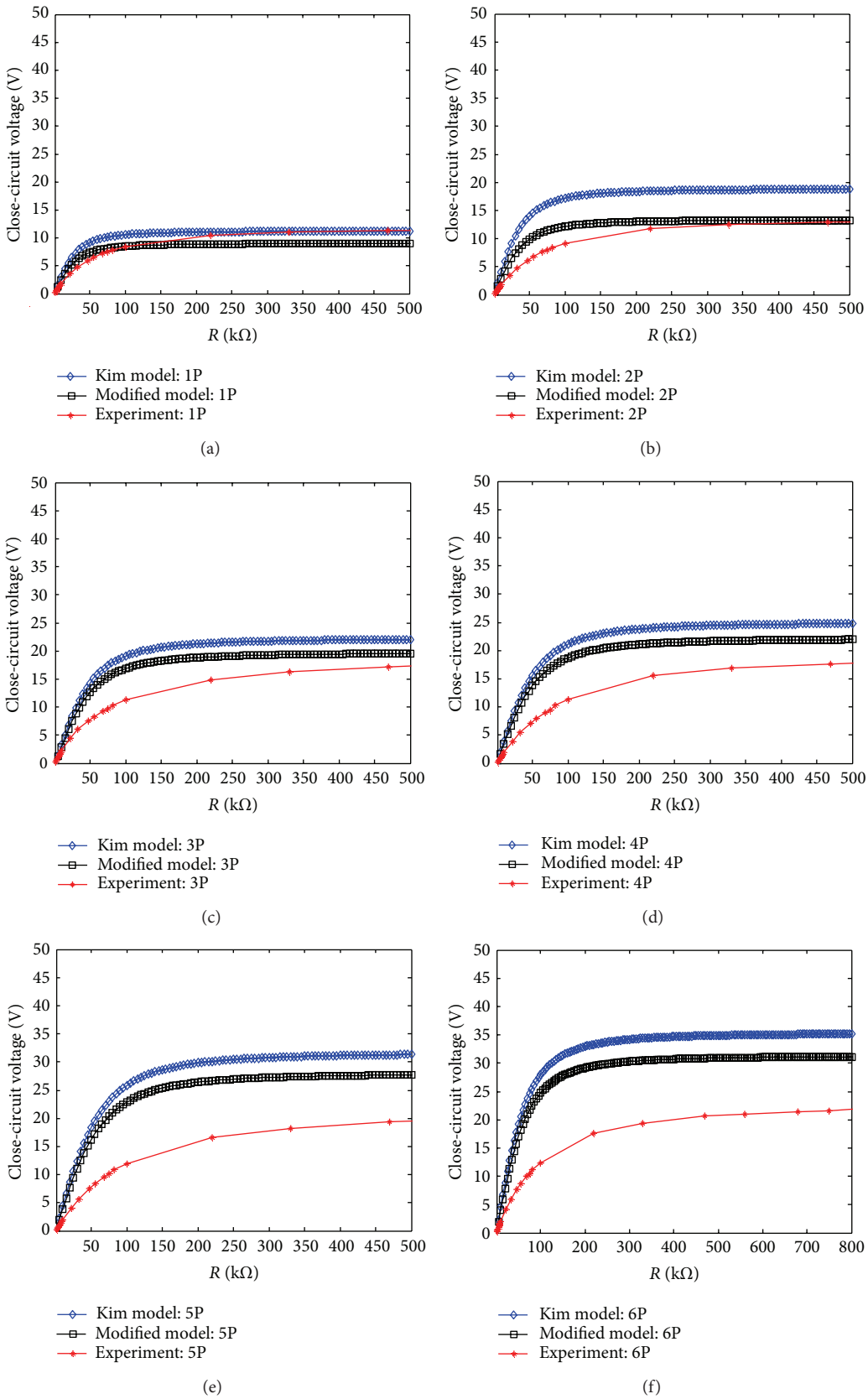

Figure 10: Resistive load voltage of Kim's model and the enhanced model.

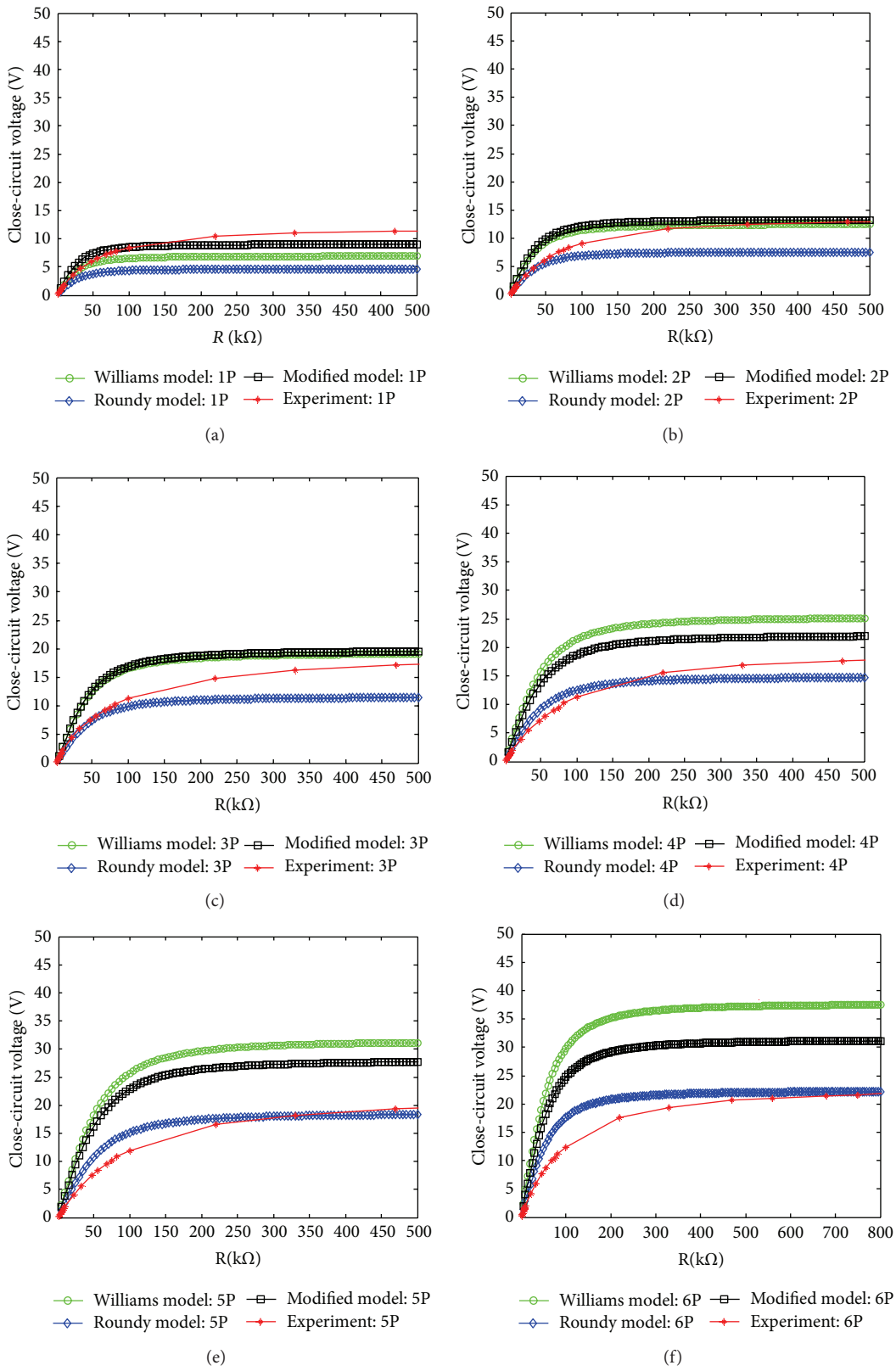

Figure 11: Resistive load voltage of Williams model, Roundy model, and the enhanced model.

the enhanced coupled field model has better accuracy in predicting the open-circuit voltage output of PCB generator with proof mass on the free end.

4.2. Close-Circuit Voltage. Under the condition that the PCB energy harvester connects with the resistive load, ranging from $1\,\Omega$ to $1\,\mathrm{M}\Omega$, the close-circuit voltage amplitude is plotted in Figure 10, comparing the theoretical results of the base model of Kim's derivation in the literature and the enhanced coupled field model against the experimental results, which are carried out with the PCB generator with 6 different proof mass attachments.

It can be seen that the enhanced coupled field model has better accuracy in predicting the close-circuit voltage of the PCB generator with different proof mass, due to that the enhanced coupled field model treats the PZT parts under the proof mass only as the rigid body without piezoelectric effect.

The enhanced coupled field model was also compared with Williams' model and Roundy's model, that is, mechanical equivalent model and electrical equivalent model, in terms of the close-circuit voltage amplitude, as shown in Figure 11. It can be seen that the enhanced coupled field model and the electrical equivalent model can better predict the close-circuit voltage output of PCB generator, while the deviation between the theoretical models and the experimental results may attribute to the internal resistance and capacitance of the PZT bimorph, geometric irregularity of the proof mass and tip displacement of the proof mass center, and so forth.

5. Conclusion

In this paper, an enhanced coupled field model based on a previous model in the literature using a conservation of energy method for the open-circuit and close-circuit voltage of PCB energy harvester has been developed with treating the PZT parts under the proof mass only as the rigid body without piezoelectric effect. The enhanced coupled field modeling is then compared with the base model and the other two previous analytical models, that is, mechanical equivalent model and electric equivalent model. Finally, the laboratory experiment is carried out to verify the enhanced coupled field model. The result shows that the enhanced coupled field model can better predict both the open-circuit voltage and the close-circuit voltage of piezoelectric cantilever bimorph generator with proof mass on the free end.

Disclosure

A portion of this work was presented at the First International Conference on Engineering and Technology Innovation, Kenting, Taiwan, 2011.

References

[1] H. A. Sodano, D. J. Inman, and G. Park, "A review of power harvesting from vibration using piezoelectric materials," *Shock and Vibration Digest*, vol. 36, no. 3, pp. 197–205, 2004.

[2] M. Rahimi, H. Shah, G. S. Sukhatme, J. Heideman, and D. Estrin, "Studying the feasibility of energy harvesting in a mobile sensor network," in *Proceedings of the IEEE International Conference on Robotics and Automation*, pp. 19–24, September 2003.

[3] A. Kansal, J. Hsu, S. Zahedi, and M. Srivastava, "Power management in energy harvesting sensor networks," *ACM Transactions on Embedded Computing Systems*, vol. 6, no. 4, article 32, 2006.

[4] L. Mateu and F. Moll, "Review of energy harvesting techniques and applications for microelectronics," in *VLSI Circuits and Systems II*, vol. 5837 of *Proceedings of SPIE*, pp. 359–373, May 2005.

[5] S. Roundy, "On the effectiveness of vibration-based energy harvesting," *Journal of Intelligent Material Systems and Structures*, vol. 16, no. 10, pp. 809–823, 2005.

[6] S. Roundy, E. S. Leland, J. Baker et al., "Improving power output for vibration-based energy scavengers," *IEEE Pervasive Computing*, vol. 4, no. 1, pp. 28–36, 2005.

[7] H. Sodano, D. Inman, and G. Park, "A review of power harvesting using piezoelectric materials (2003–2006)," *Smart Materials and Structures*, vol. 16, no. 2, pp. 1–21, 2007.

[8] S. Priya, "Advances in energy harvesting using low profile piezoelectric transducers," *Journal of Electroceramics*, vol. 19, no. 1, pp. 165–182, 2007.

[9] C. B. Williams and R. B. Yates, "Analysis of a micro-electric generator for microsystems," *Sensors and Actuators A*, vol. 52, no. 3, pp. 8–11, 1996.

[10] C. H. Park, "On the circuit model of piezoceramics," *Journal of Intelligent Material Systems and Structures*, vol. 12, no. 7, pp. 515–522, 2001.

[11] S. Roundy and P. K. Wright, "A piezoelectric vibration based generator for wireless electronics," *Smart Materials and Structures*, vol. 13, no. 5, pp. 1131–1142, 2004.

[12] Q. M. Wang, X. H. Du, B. Xu, and L. E. Cross, "Theoretical analysis of the sensor effect of cantilever piezoelectric benders," *Journal of Applied Physics*, vol. 85, no. 3, pp. 1702–1712, 1999.

[13] Q. M. Wang and L. Eric Gross, "Constitutive equations of symmetrical triple layer piezoelectric benders," *IEEE Transactions on Ultrasonics, Ferroelectrics, and Frequency Control*, vol. 46, no. 6, pp. 1343–1351, 1999.

[14] S. Kim, *Low power energy harvesting with piezoelectric generators [Ph.D. thesis]*, University of Pittsburgh, 2002.

[15] T. H. Ng and W. H. Liao, "Sensitivity analysis and energy harvesting for a self-powered piezoelectric sensor," *Journal of Intelligent Material Systems and Structures*, vol. 16, no. 10, pp. 785–797, 2005.

[16] J. Ajitsaria, S. Y. Choe, D. Shen, and D. J. Kim, "Modeling and analysis of a bimorph piezoelectric cantilever beam for voltage generation," *Smart Materials and Structures*, vol. 16, no. 2, pp. 447–454, 2007.

[17] Information on, http://www.piezo.com/prodmaterialprop.html.